On the Steady Performance of Annular Hydrostatic Thrust Bearing: Rabinowitsch Fluid Model

Udaya P. Singh[1]
Associate Professor of Mathematics,
Department of Applied Science,
Ambalika Institute of Management & Technology,
Lucknow, 227305 Uttar Pradesh, India
e-mail: journals4phd@gmail.com

Ram S. Gupta
Professor of Mathematics,
Department of Applied Science,
Kamala Nehru Institute of Technology,
Sultanpur, 228118 Uttar Pradesh, India

Vijay K. Kapur
Former Professor and Head,
Department of Applied Science,
Kamala Nehru Institute of Technology,
Sultanpur, 228118 Uttar Pradesh, India

The present theoretical analysis investigates the simultaneous effect of lubricant inertia and non-Newtonian pseudoplastic lubricant (lubricant blended with viscosity index improver and viscosity thickener)–Rabinowitsch fluid model on the performance of externally pressurized annular hydrostatic thrust bearings. A close form solution is obtained for pressure distribution. The effect of centrifugal inertia on the pressure distribution in the recess region is considered by taking non-constant recess pressure under a hydrodynamic condition. The load capacity and flow rate have been numerically calculated for various values of viscosity index improver together with the centrifugal inertia effects. In the limiting case in which there is an absence of pseudoplasticity, the results are compared with the pre-established Newtonian lubricants and are found to be in good agreement. [DOI: 10.1115/1.4007350]

Keywords: fluid film lubrication, hydrostatic lubrication, pressurized bearings, thrust bearings, Rabinowitsch fluid model

1 Introduction

An annular hydrostatic thrust bearing is a type of hydrostatic bearing or externally pressurized bearing system. Due to the potential advantages of hydrostatic thrust bearings, several investigations have been presented by the researchers from time to time on design and lubricant effects on the performance of hydrostatic bearing systems [1–3], the effect of lubricant inertia and temperature [4–6], and dynamic characteristics including fluid compressibility [7]. Chow [8] presented the concept of annular recess hydrostatic thrust bearings to avoid cavitation and increase the stability and life of the bearing, and recently the problem of annular hydrostatic thrust bearings has been analyzed by Bakker and Ostayen [9] and the optimized recess depth was presented for Newtonian fluids.

On the other hand, tribologists have also done a great deal of work to increase the efficiency of stabilizing properties of non-Newtonian lubricants through the addition of long chain polymer solutions (polyisobutylene and ethylene propylene etc.) as viscosity index improvers. The use of additives minimize the sensitivity of the lubricant to the change in the shearing strain rate for which many non-Newtonian models such as couple stress, power law, micropolar, and Casson models are of common use. Among these models, the Rabinowitsch fluid model [1,10] is an established model [10] to analyze the non-Newtonian behavior of the fluid. Wada and Hayashi [10] showed that the lubricants blended with viscosity index improver behave like pseudoplastic fluids which can be analyzed by the Rabinowitsch fluid model given by the following relation for one dimensional fluid flow:

$$\bar{\tau}_{rz} + \kappa\bar{\tau}_{rz}^3 = \bar{\mu}\frac{\partial \bar{u}}{\partial \bar{z}} \tag{1}$$

where $\bar{\mu}$ is the *initial viscosity* and κ is the nonlinear factor responsible for the non-Newtonian effects of the fluid, which will be referred to as coefficient of pseudoplasticity in this paper. This model can be applied to Newtonian lubricants for $\kappa = 0$, to dilatant lubricants for $\kappa < 0$, and to pseudoplastic lubricants for $\kappa > 0$. The advantage of this model lies in the fact that the theoretical analysis for this model is verified with the experimental justification by Wada and Hayashi [10]. After Wada and Hayashi, many researchers used this model for the theoretical study of bearing performance with non-Newtonian lubricants [11–13]. Recently, this model was used by Singh et al. [1,14] to analyze the performance of circular and curvilinear hydrostatic thrust bearings and Lin [15] to analyze the performance of annular squeeze film bearings.

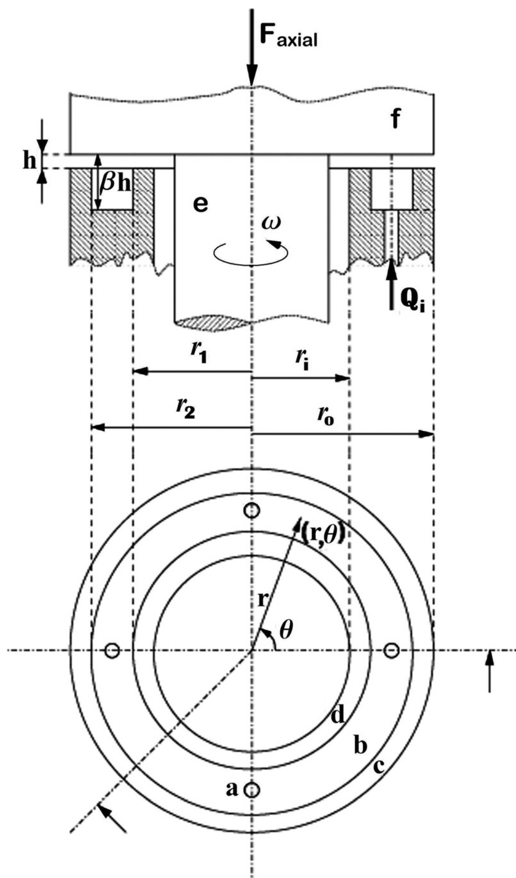

Fig. 1 Schematic diagram of annular thrust bearing with (*a*) inlet hole, (*b*) recess, (*c*) outer land, (*d*) inner land, (*e*) shaft, and (*f*) collar

[1]Corresponding author.

Contributed by the Tribology Division of ASME for publication in the Journal of Tribology. Manuscript received June 16, 2012; final manuscript received August 2, 2012; published online August 24, 2012. Assoc. Editor: George K. Nikas.

The objective of the present paper is to extend the results of the Rabinowitsch model [1,14] to the hydrostatic annular thrust bearings.

2 Analysis

The physical configuration of an externally pressurized annular thrust bearing is shown in Fig. 1. The lubricant in the system is taken as a non-Newtonian pseudoplastic fluid. The body forces and body couples are considered to be absent and the assumptions of thin film lubrications are assumed to be applicable. After Singh et al. [1], the modified Reynolds equation in the present problem is obtained as:

$$\frac{1}{\bar{r}}\frac{d}{d\bar{r}}\left[\frac{\bar{r}\bar{h}^3}{12\bar{\mu}}\left(\bar{f}+\frac{3\kappa\bar{h}^2}{20}\bar{f}^3\right)\right]=0 \tag{2}$$

where

$$\bar{f}=\frac{1}{\bar{h}}\int_0^{\bar{h}}\left(\frac{\partial\bar{p}}{\partial\bar{r}}-\frac{\rho\bar{v}^2}{r}\right)d\bar{z}=\frac{\partial\bar{p}}{\partial\bar{r}}-\frac{\rho\bar{r}\omega^2}{3}\quad\text{and}\quad\bar{v}=\bar{r}\omega\frac{\bar{z}}{\bar{h}}$$

The modified Reynolds equation (Eq. (2)) takes the dimensionless form:

$$\frac{1}{r}\frac{d}{dr}\left[\frac{rh^3}{12\mu}\left(f+\tilde{\alpha}f^3\right)\right]=0 \tag{3}$$

where $\tilde{\alpha}=\frac{3\alpha h^2}{20}$ and $f=\frac{\partial p}{\partial r}-\frac{1}{3}Sr$.

As the Reynolds equation (Eq. (3)) is a nonlinear equation in pressure p, it is not easy to solve it using analytical methods. Therefore, the classical perturbation method is used to solve it.

The perturbation series for the pressure distribution p can be expressed in the form

$$p(r)=p_o(r)+\tilde{\alpha}p_1(r)+\tilde{\alpha}^2p_2+\mathrm{O}(\tilde{\alpha}^3) \tag{4}$$

For $\tilde{\alpha}\ll 1$ (Table 3), it is sufficient to consider

$$p(r)=p_o(r)+\tilde{\alpha}p_1(r) \tag{5}$$

Substituting Eq. (5) in Eq. (3), the perturbed form of the Reynolds equation is obtained as:

$$\frac{1}{r}\frac{d}{dr}\left[\frac{rh^3}{12\mu}\left(\frac{dp_o}{dr}-\frac{1}{3}Sr\right)\right]=0 \tag{6}$$

$$\frac{1}{r}\frac{d}{dr}\left[\frac{rh^3}{12\mu}\left\{\frac{dp_1}{dr}+\left(\frac{dp_o}{dr}-\frac{1}{3}Sr\right)^3\right\}\right]=0 \tag{7}$$

Integrating equations (Eqs. (6)–(7)), the expression for pressure distribution is obtained as

$$p_o(r)=\frac{1}{6}Sr^2+c_{01}\log(r)+c_{02} \tag{8}$$

$$p_1(r)=c_{11}\log(r)+\frac{c_{01}^3}{2}\frac{1}{r^2}+c_{12} \tag{9}$$

In order to evaluate coefficients appearing in Eqs. (8)–(9), the pressure is individually evaluated in the three regions of the bearing: the inner region, the recess region and the outer region (Fig. 1). After Bakker and Ostayen [9], the pressure distribution including centrifugal inertia effect is evaluated in two steps as follows.

Step 1: For $S=0$, the values of the coefficients in Eqs. (8)–(9) are evaluated under boundary condition $p=0$ at $r=r_i$ and $r=1$, to find the general solution (p_G) of the Reynolds equation. In this case, the pressure in the recess equals a fraction of the supply pressure $\left(\beta_pP_o:0<\beta_p<1\right)$. The pressure distribution is given as

$$p_G=\begin{cases}b_{101}\log(r)+b_{102}+\frac{3}{20}\alpha h^2\left(b_{111}\log(r)+\frac{b_{101}^3}{2}\frac{1}{r^2}+b_{112}\right); & r_i\le r\le r_1\\ \beta_p; & r_1\le r\le r_2\\ b_{201}\log(r)+b_{202}+\frac{3}{20}\alpha h^2\left(b_{211}\log(r)+\frac{b_{201}^3}{2}\frac{1}{r^2}+b_{212}\right); & r_2\le r\le 1\end{cases} \tag{10}$$

where, the coefficients b_{01} through b_{21} can be found in Appendix B.

Step 2: For $S>0$, the coefficients in Eqs. (8)–(9) are evaluated under the hydrodynamic condition, considering the hydrodynamic pressure built up by the centrifugal inertia effects only, to obtain a particular solution p_I of the Reynolds equation.

$$p_I=\begin{cases}\frac{1}{6}Sr^2+c_{101}\log(r)+c_{102}+\frac{3}{20}\alpha h^2\left(c_{111}\log(r)+\frac{c_{101}^3}{2}\frac{1}{r^2}+c_{112}\right); & r_i\le r\le r_1\\ \frac{1}{6}Sr^2+c_{201}\log(r)+c_{202}+\frac{3}{20}\alpha h^2\left(c_{211}\log(r)+\frac{c_{201}^3}{2}\frac{1}{r^2}+c_{212}\right); & r_1\le r\le r_2\\ \frac{1}{6}Sr^2+c_{301}\log(r)+c_{302}+\frac{3}{20}\alpha h^2\left(c_{311}\log(r)+\frac{c_{301}^3}{2}\frac{1}{r^2}+c_{312}\right); & r_2\le r\le 1\end{cases} \tag{11}$$

where, the coefficients c_{101} through c_{312} are evaluated under the six boundary conditions: $p_I=0$ at $r=r_i$ and $r=1$, continuity of pressure at the steps $r=r_1$ and $r=r_2$, and continuity of lubricant flow at the steps $r=r_1$ and $r=r_2$. The expressions for the coefficients c_{101}, c_{102}, c_{111}, c_{112}, c_{201}, c_{202}, c_{211}, c_{212}, c_{301}, c_{302}, c_{311}, and c_{312} are not presented in the analysis due to limited utility.

It is expected that the overall pressure distribution $P(p_G+p_I)$ will be a realistic estimate of the effects of centrifugal inertia and pseudoplasticity.

3 Load Carrying Capacity and Lubricant Flow-Rate

After, Singh et al. [1], the dimensionless load carrying capacity W and the dimensionless flow rate Q are given by

$$W = 2\left(\int_{r_i}^{r_1} rpdr + \int_{r_1}^{r_2} rpdr + \int_{r_2}^{1} rpdr\right) \tag{12}$$

$$Q = -\frac{rh^3}{\mu}\left(f + \frac{3}{20}\alpha h^2 f^3\right) \tag{13}$$

where 'f' is found in Eq. (3).

4 Results and Discussions

To study the centrifugal inertia effects in case of non-Newtonian (pseudoplastic) lubricants on the steady performance of externally pressurized annular thrust bearing, the numerical results for pressure, load capacity, and radial flow rate have been obtained for the different values of parameter of pseudoplasticity, $\alpha(\alpha = \kappa P_o^2)$. For the practical applicability of the problem, the experimental values for coefficient of pseudoplasticity, $\kappa = 0$ (classical Newtonian fluids), $\kappa = 5.65 \times 10^{-6}$ m^4/N^2 (0.3% additive), and 3.05×10^{-6} m^4/N^2 (1% additive) obtained by Wada and Hayashi [10] have been used (Table 2) in the discussions. Furthermore, the theoretical results of pressure, load capacity and radial flow rate for the Newtonian and non-Newtonian (pseudoplastic) lubricants have been compared with the results of Bakker and Ostayen [9] for different values of rotation parameter S, in Figs. 2–4, to justify the present analysis. It was observed that the results (pressure, load capacity, and radial flow rate) for Newtonian fluids ($\kappa = 0$) in the present analysis are the same as those obtained by Bakker and Ostayen [9].

For the numerical calculation and discussions of the results, dimensionless film thickness $h = 0.003$, film thickness ratio $\beta = 2$, 5, and parameter of centrifugal inertia $S = 0$, 1.0, 2.0 are taken [1] in the analysis.

In Fig. 2, the variation of dimensionless pressure (P) with respect to the radius of the bearing is shown for $\beta = 2$. The pressure for Newtonian lubricants ($\kappa = 0$) is higher than the pressure for pseudoplastic lubricants and pressure also decreases with the increase of viscosity index improver (i.e. decrease of pseudoplasticity κ) even if the viscosity increases (Table 2). That is, the pressure for pseudoplastic lubricants increases with the increase of κ but below the Newtonian pressure: a result in agreement with the results of Singh et al. [1] and experimental results of Wada and Hayashi [10]. It is further concluded that the effect of additive (pseudoplasticity) on pressure distribution is small in the case of

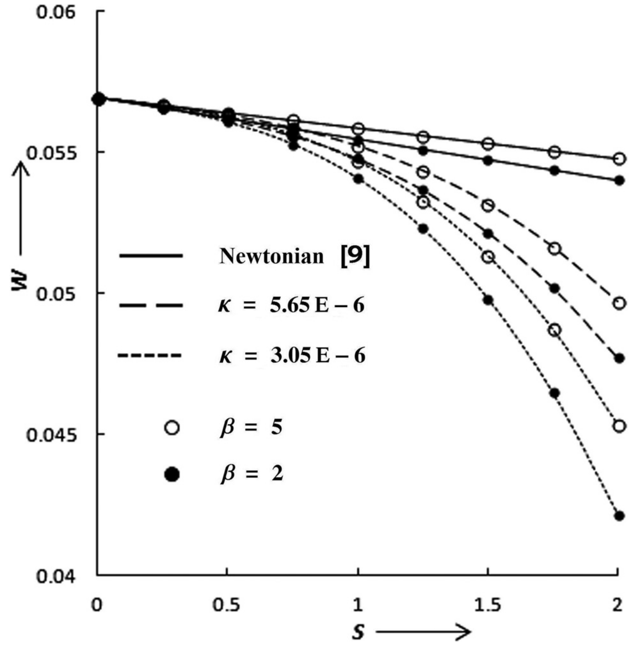

Fig. 3 Variation of load capacity (W) with S. Dimension of κ is in m^4/N^2 [10].

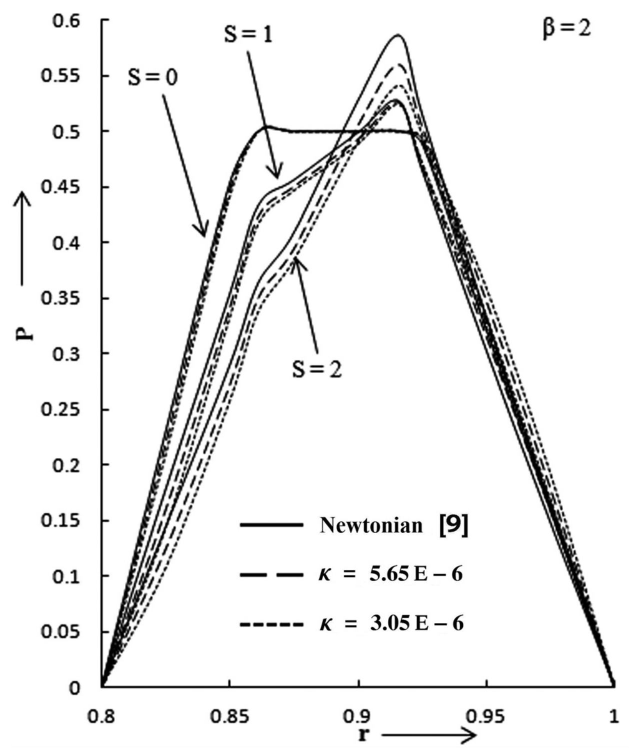

Fig. 2 Variation of pressure with radius. Dimension of κ is in m^4/N^2 [10].

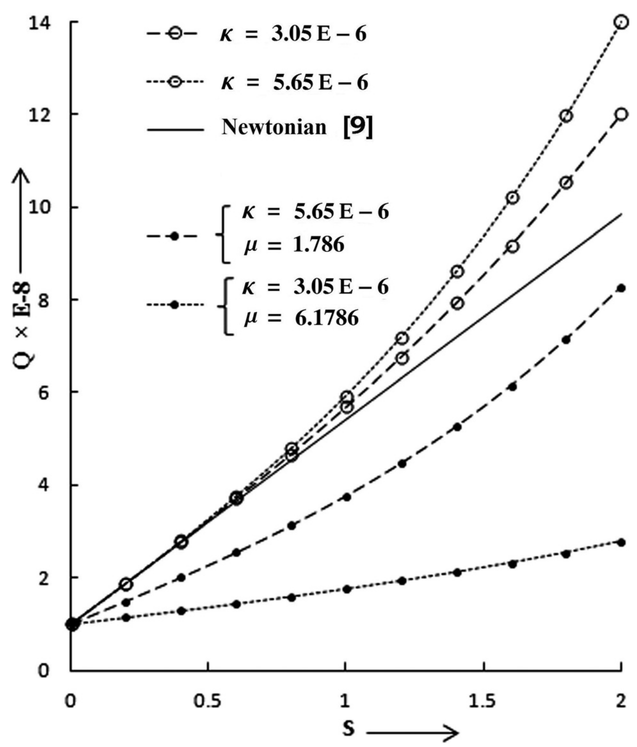

Fig. 4 Variation of lubricant flow rate (Q) with S for $\beta = 2$. Dimension of κ is in m^4/N^2 [10].

Table 1 Maximum variation (decrease) of pressure (P) and variation (decrease) of load (W) from newtonian results [9]. $\beta = 2$.

S / κ (m^4/N^2)	0		1		2	
	P	W	P	W	P	W
5.65×10^{-6}	4.54%	0.12%	8.24%	2.13%	16.01%	11.03%
3.05×10^{-6}	7.06%	0.67%	14.32%	9.15%	25.62%	19.31%
2.95×10^{-6}	7.38%	0.94%	17.12%	12.10%	27.11%	21.07%

Note: Data for κ taken from the experimental result of Wada and Hayashi [10].

no rotation (S = 0), but in the case of high values of centrifugal inertia "S" (i.e. the case of high rotation or large radius), the deviation of pressure distribution for pseudoplastic lubricant from Newtonian case can be easily observed. It can be explained as the effect of increasing the rotation and hence the centrifugal inertia decreases the shearing stress. A comparative analysis of combined effects of pseudoplasticity (κ) and centrifugal inertia (S) on pressure is obtained in Table 1.

Figure 3 shows the variation of dimensionless load capacity with respect to the inertia parameter S for thickness ratio $\beta = 2, 5$ and coefficient of pseudoplasticity $\kappa = 0,\ 5.65 \times 10^{-6}$, $3.05 \times 10^{-6} m^4/N^2$ [10]. The variation of dimensionless load capacity with κ is similar with the pressure. It is observed that for each value of rotation parameter S and thickness ratio β, the dimensionless load capacity for Newtonian fluid ($\kappa = 0$) is higher than that for the pseudoplastic fluids ($\kappa > 0$) and the load capacity for pseudoplastic lubricants increases with κ. However, upon careful observation of Figs. 3 and Table 1, it can be concluded that the deviation of load carrying capacity for pseudoplastic lubricants is small in the case of no rotation ($S = 0$) but in the case of high rotation or large radius (i.e. increase in the value of centrifugal effect (S)), the deviation of load carrying capacity for pseudoplastic lubricants is significant, which is similar with the variation of pressure. This can also give a direction and a guideline for better bearing analysis and design.

In Fig. 4, the variation of dimensionless radial flow-rate with respect to S is shown for the two cases; first, when the viscosity does not change but pseudoplasticity (κ) varies ($\mu = \bar{\mu}/\mu_n = 1$), the flow characteristics are plotted with blank circles and second, when viscosity varies due to additives with the pseudoplasticity ($\mu = \bar{\mu}/\mu_n > 1$) (see Table 2), the flow characteristics are plotted with the solid circles. In the first case (no variation of viscosity), the flow rate for pseudoplastic fluids is higher than the Newtonian fluids and the flow rate also increases with the decrease of κ. While in the second case, when the viscosity increases with the amount of additive (Table 2), the flow rate decreases with the increase of viscosity regardless of the value of pseudoplasticity κ. Since, in the real situation, the viscosity of the base oil (Newtonian lubricant) increases with the amount of additive [10], the dimensionless flow-rate for the 'lubricants with additives' will be always less than the base (Newtonian) oil and it will also decrease with the amount of additive. However, if it is possible to keep the viscosity of the base oil unaltered with the blending of additives (viscosity index improvers), the flow rate of these lubricants will be higher than the base oil and it will increase with κ (pseudoplastic parameter) where κ can be determined experimentally [10].

5 Conclusion

The pseudoplastic effect of an isothermal incompressible non-Newtonian lubricant on the steady performance of annular thrust bearing is presented.

Based on the present analysis, the following conclusions are drawn:

(1) In comparison to the Newtonian case, the film pressure with the pseudoplastic lubricants is lower. Furthermore, there is a significant decrease in the pressure and load capacity by decreasing the pseudoplastic coefficient κ [1].
(2) The effect of pseudoplasticity on the pressure and load capacity of the bearing is small in the case of 'no rotation' and it relatively increases with the rotation due to centrifugal inertia effect (S) [1].
(3) The effect of additive (viscosity index improver) is attributable to pressure and hence to load capacity due to the change of the lubricant's nature from Newtonian (base oil) to pseudoplastic [1].
(4) In comparison with the Newtonian lubricant (base oil), the flow rate increases with the increase of pseudoplasticity while it decreases with the increase of viscosity. However, the major effect of an additive (viscosity index improver) on the flow rate is due to the viscosity variation [1].

Nomenclature

$f = \frac{\bar{f}R}{P_o}$
$\bar{h}, h =$ film thickness, $h = \frac{\bar{h}}{R}$
$\bar{p}, p =$ film pressure, $p = \frac{\bar{p}}{P_o}$
$P_o =$ supply pressure
$\overline{Q}, Q =$ radial flow rate, $Q = \frac{6\mu_n \overline{Q}}{\pi R^3 P_o}$
$\bar{r}_1, \bar{r}_2 =$ recess radii
$r_1, r_2 = \frac{\bar{r}_1}{R}, \frac{\bar{r}_2}{R}$
$\bar{r}_i, r_i =$ inner radius, $r_i = \frac{\bar{r}_i}{R}$
$r = \frac{\bar{r}}{R}$
$R =$ bearing outer radius
$s = \frac{3}{20} \frac{\rho R^2 \omega^2}{P_o}$
$\bar{u} =$ radial velocity of the fluid
$u = \frac{\bar{u}}{r\omega}$
$\bar{v} =$ circumferential velocity
$v = \frac{\bar{v}}{r\omega}$
$W = \frac{\bar{W}}{\pi R^2 P_o}$
$\bar{W} =$ load capacity
$\alpha = \kappa P_o^2$
$\tilde{\alpha} = \frac{3\alpha h^2}{20}$
$\beta =$ film thickness ratio
$\beta_p =$ fraction of supply pressure
$\kappa =$ coefficient of pseudoplasticity
$\mu = \frac{\bar{\mu}}{\mu_n}$
$\bar{\mu} =$ viscosity of the fluid blended with viscosity index improver
$\mu_n =$ viscosity of base fluid
$\rho =$ density of fluid
$\tau = \frac{\bar{\tau}}{2\pi\mu_N R^2 \omega}$
$\omega =$ angular velocity of runner

Appendix A

Table 2 Lubricants additive

Additives %	T(°C)	(Pa · s)	$\mu = \bar{\mu}/\mu_n$	κ(m^4/N^2)
0	25	0.140 (μ_n)	1	0
0.3	22	0.250	1.786	5.65×10^{-6}
1.0	22	0.610	4.357	3.05×10^{-6}
2.0	25	0.865	6.1786	2.95×10^{-6}

Note: Data are from the experimental result of Wada and Hayashi [10].

Table 3 Calculation of dimensionless parameter $\tilde{\alpha}$

$\bar{h}(m)$	R (m)	$h(\bar{h}/R)$	P_o(Pa)	$\kappa(\mathrm{m}^4/\mathrm{N}^2)$	$\alpha(\kappa P_0^2)$	$\tilde{\alpha}(3\alpha h^2/20)$
0.002	0.5	0.004	10^4	0	0	0
0.002	0.5	0.004	10^4	5.65×10^{-6}	565	0.001356
0.002	0.5	0.004	10^4	3.05×10^{-6}	305	0.000732
0.002	0.5	0.004	10^4	2.95×10^{-6}	295	0.000708

Note: Present data are taken for numerical calculations. However, analysis is valid for any set of values of $\bar{h}$, R, κ and P_o, which satisfy the condition $\tilde{\alpha} \ll 1$.

Appendix B

Coefficient for $S = 0$

$$b_{101} = \frac{\beta_p}{\mu\{\log(r_1) - \log(r_i)\}}; \quad b_{102} = -\frac{\beta_p \log(r_i)}{\log(r_1) + \log(r_i)}$$

$$b_{111} = \frac{r_1^2\beta_p^3 - r_i^2\beta_p^3}{2r_1^2 r_i^2\mu^3\{\log(r_1) - \log(r_i)\}^4};$$

$$b_{112} = -\frac{r_1^2\beta_p^3\log(r_1) - r_i^2\beta_p^3\log(r_i)}{2r_1^2 r_i^2\mu^2\{\log(r_1) - \log(r_i)\}^4}$$

$$b_{201} = \frac{\beta_p}{\mu\log(r_2)}; \quad b_{202} = 0$$

$$b_{211} = -\frac{\beta_p^3 - r_2^2\beta_p^3}{2r_2^2\mu^3\log(r_2)^4}; \quad b_{212} = -\frac{\beta_p^3}{2\mu^2\log(r_2)^3}$$

References

[1] Singh, U. P., Gupta, R. S., and Kapur, V. K., 2011, "On the Steady Performance of Hydrostatic Thrust Bearing: Rabinowitsch Fluid Model," Tribol. Trans., **54**(5), pp. 723–729.

[2] Hamrock, B. J., Schmid, S. R., and Jacobson, B. O., 2004, *Fundamentals of Fluid Film Lubrication*, 2nd ed., Marcel Dekker, New York.

[3] Bassani, R., and Piccigallo, B., 1992, *Hydrostatic Lubrication*, Elsevier, Amsterdam.

[4] Coombs, J. A., and Dowson, D., 1964, "An Experimental Investigation of the Effects of Lubricant Inertia in a Hydrostatic Thrust Bearing," Proc. Inst. Mech. Eng., London, **179**, pp. 96–108.

[5] Peterson, J., Finn, W. E., and Dareing, D. W., 1994, "Non-Newtonian Temperature and Pressure Effects of a Lubricant Slurry in Rotating Hydrostatic Step Bearing," Tribol. Trans., **37**(4), pp. 857–863.

[6] Kapur, V. K., and Verma, K., 1979, "The Simultaneous Effects of Inertia and Temperature on the Performance of a Hydrostatic Thrust Bearing," Wear, **54**(1), pp. 113–122.

[7] Lin, J. R., 1999, "Static and Dynamic Characteristics of Externally Pressurized Circular Step Thrust Bearings Lubricated With Couple Stress Fluids," Tribol. Int., **32**, pp. 207–216.

[8] Chow, C.-Y., 1975, "A Non-Central Feeding Hydrostatic Thrust Bearing," J. Fluid Mech., **72**, pp. 113–120.

[9] Bakker, O. J., and Ostayen, R. A. J., 2010, "Recess Depth Optimization for Rotating, Annular, and Circular Recess Hydrostatic Thrust Bearings," ASME J. Tribol., **132**, pp. 1–7.

[10] Wada, S., and Hayashi, H., 1971, "Hydrodynamic Lubrication of Journal Bearings by Pseudoplastic Lubricants (Part II, Experimental Studies)," Bull. JSME, **14**(69), pp. 279–286.

[11] Bourging, P., and Gay, B., 1984, "Determination of the Load Capacity of Finite Width Journal Bearing by Finite Element Method in the Case of a Non-Newtonian Lubricant," ASME J. Tribol., **106**, pp. 285–290.

[12] Hashmimoto, H., and Wada, S., 1986, "The Effects of Fluid Inertia Forces in Parallel Circular Squeeze Film Bearing Lubricated With Pseudoplastic Fluids," ASME J. Tribol., **108**, pp. 282–287.

[13] Lin, J. R., 2001, "Non-Newtonian Effects on the Dynamic Characteristics of One Dimensional Slider Bearings: Rabinowitsch Model," Tribol. Lett., **10**(4), pp. 237–243.

[14] Singh, U. P., Gupta, R. S., and Kapur, V. K., 2011, "Effects of Inertia in the Steady State Pressurised Flow of a Non-Newtonian Fluid Between Two Curvilinear Surfaces of Revolution: Rabinowitsch Fluid Model," Chem. Process Eng., **32**(4), pp. 333–349.

[15] Lin, J.-R., 2012, "Non-Newtonian Squeeze Film Characteristics Between Parallel Annular Disks: Rabinowitsch Fluid Model," Tribol. Int., **52**, pp. 190–194.